ELSEVIER

Journal of Molecular Catalysis A: Chemical 134 (1998) 145–157

JOURNAL OF MOLECULAR CATALYSIS A: CHEMICAL

Butene oligomerization over mesoporous MTS-type aluminosilicates

B. Chiche [a], E. Sauvage [a], F. Di Renzo [a], I.I. Ivanova [a,b], F. Fajula [a,*]

[a] *Laboratoire de Matériaux Catalytiques et Catalyse en Chimie Organique, UMR 5618 CNRS, ENSCM, 8 Rue de l'Ecole Normale, 34296 Montpellier Cedex 5, France*

[b] *Laboratory of Kinetics and Catalysis, Department of Chemistry, Moscow State University, Vorob'evy Gory, 117234 Moscow, Russian Federation*

Received 27 August 1997; accepted 9 October 1997

Abstract

The oligomerization of butene at 423 K and 1.5–2 MPa has been investigated over a series of zeolite, amorphous silica–alumina (ASA) and ordered mesoporous aluminium-containing micelle templated silica (MTS) catalysts. While olefin oligomerization into strongly adsorbed residue and fast deactivation prevailed on microporous catalysts and ASA, mesoporous aluminosilicates with uniform pore openings near 3 nm in size exhibited high selectivity and good stability with time for the production of branched dimers. The characterization of the surface properties of the solids, the nature of the adsorbed residue on the spent catalysts, and the identification of reaction intermediates by in situ infrared spectroscopy of co-adsorbed acetonitrile and butene, suggest that the unique catalytic behaviour of MTS-type catalysts is related to the moderate strength and the high dispersion of the acid sites in the mesoporous structure.

Keywords: Mesoporous aluminosilicates; Zeolites; Silica–alumina; Butene oligomerization; Acidity; Texture

1. Introduction

Micelle templated silicas (MTS) constitute a new class of inorganic molecular sieves with well-controlled narrow pore size distributions that can be tuned in the 1.5–10 nm range. Since the first reports by researchers from Mobil and Waseda University [1–5] on the synthesis of this family of materials prepared via a self assembly process, where positively charged quaternary ammonium surfactant micelles act as templates for the negatively charged silicate network, many related materials have been generated (M41S [1], HMS [6], TMS [7], MMS [8], SBA [9], MSU [10], PCH [11], FSM [4]) by using a variety of cationic, anionic or neutral surfactants.

With regards to catalytic applications, the MCM-41 member of the M41S family has been the most extensively studied to date. Active catalytic centres can be created by inserting aluminium [1,8], vanadium [12], titanium [13–15], manganese [16], iron [17,18], gallium [17–19], chronium [20] and boron [12] into the silicate network, imparting acidic or redox proper-

* Corresponding author.

1381-1169/98/$19.00
PII: S1381-1169(98)00031-4

ties. In the case of aluminium incorporation, Brönsted and Lewis sites are created, as it is usually observed for amorphous and crystalline aluminosilicates. The surface acidity of MTS-type materials has been often described on the bases of models developed in the field of zeolite science. It must be stressed however that the surfaces of the two kinds of materials differ significantly. First, the inner surface of a zeolite is limited by a completely connected network of tetrahedra, whereas the inner surface of MTS interrupts a framework of amorphous silica–alumina and is essentially lined by hydroxyl groups. This situation leads to a rather flexible framework in MTS in comparison to the rigid zeolite networks. Second, the peculiar synthesis mechanism of MTS, where the single-charged aluminate anions preferentially react with the silica layer already coating the micelles, severely restricts the incorporation of aluminium at the surface, limiting therefore the number of acid sites accessible to the reagents. Previous spectroscopic characterizations of materials prepared with widely varying compositions led to the conclusion that no more than 1 aluminium per 60 tetrahedra was measured at the surface using usual basic probes [21,22].

On the other hand, MTS differ also from amorphous silica–aluminas because of a more uniform dispersion of the acid sites on the surface of the former, owing to their formation mechanism (vide supra) and to the surface areas attained.

In view of the peculiarities of their textural and acidic characteristics, mesoporous solid acid catalysts have opened new perspectives for the synthesis and conversion of large molecules unable to enter the micropores of zeolites. Examples of such applications have been indeed reported [23–26] (for a review, see Ref. [27]), but amazingly, excellent activities and selectivities into gasoline and middle distillates in the oligomerization of light olefins have been also disclosed, under conditions where zeolites and classical amorphous silica–aluminas are practically inactive [17,28–30].

As the implications of porosity and acidity on activity and selectivity in the conversion of olefins have not been fully elucidated yet, we undertook a comparative study of the reaction of butene over a series of zeolites, amorphous silica–alumina, and MTS-type catalysts with different pore sizes.

2. Experimental

2.1. Catalysts

Aluminium-containing micelle templated silicas were synthesized using cetyltrimethylammonium (CTMA) or octyltrimethylammonium (OTMA) bromide (Aldrich), Aerosil 200 V (Degussa) or Zeosil 175 MP (CECA) silicas, aluminium sulfate (Aldrich), sodium hydroxide (Prolabo) and deionised water. The reagents have been mixed at 343 K under stirring in a stainless steel vessel, sealed and then heated at 393 K. The solid phase was then separated by filtration, washed first with deionized water until pH 9, then with ethanol, and dried at 353 K [22,31]. The alkali content of the samples being always negligible with respect to the Al content, acidic catalysts were prepared by calcining the as-made solids in a flow (100 ml/min) of dry air at 823 K for 7 h. The solids were then re-equilibrated with ambient moisture for at least two days.

The reference catalysts used for comparison purposes were a zeolite H-beta (hereafter BEA, $Si/Al = 26$, synthesized in the laboratory [32]), a zeolite H-ZSM-5 (hereafter MFI, $Si/Al = 25$, CBV 5020 from Conteka) and amorphous silica–alumina (hereafter ASA, 13 wt.% alumina, from Ketjen).

2.2. Sample characterization

Powder X-ray diffraction (XRD) patterns were recorded by using a CGR Thêta-60 diffractometer with monochromated Cu Kα radiation. Textural properties have been characterized by

nitrogen adsorption at 77 K, on calcined samples outgassed at 525 K, with a Micromeritics ASAP 2000 apparatus. For the MTS family of materials, the mesopore volume (V) was measured at the top of the type IV adsorption step, and pore diameters were calculated by using the formula $D_{4V/S} = 4V/S_{BET}$ [33].

The composition and nature of the carbonaceous residue was investigated by combined thermogravimetry/thermal analysis/mass spectrometry (TG/DSC/MS, Setaram DSC 111 analyzer interfaced with a Leybold Quadrex 200), by infrared (FTIR, Nicolet 320) and Diffuse Reflectance UV–Visible (UV–Vis, Perkin-Elmer Lambda 14) spectroscopies. ^{13}C MAS NMR spectra using the HP decoupling technique were recorded with a Bruker AM 300 spectrometer (300 and 75.4 MHz for ^{1}H and ^{13}C, respectively) using a 7-mm zirconia rotor spun at 3 kHz in dry air. The spectra recorded with the $^{1}H/^{13}C$ cross-polarization technique were obtained on a Bruker ASX 400 spectrometer (400 and 100.6 MHz for ^{1}H and ^{13}C, respectively) using 4 mm rotors spun at 5 kHz.

2.3. Acidity measurements and identification of intermediates

The acidity of the catalysts was studied by ammonia temperature programmed desorption (TPD) and microcalorimetry, and by infrared spectroscopy of adsorbed acetonitrile. Ammonia TPD experiments were performed using a homemade apparatus with continuous titration of the effluent gases by conductimetry. The heats of adsorption of ammonia were determined by microcalorimetry on a Tian-Calvet type calorimeter from Setaram. The details of the experimental procedures have been given recently [34].

Identification of intermediate carbenium ions in the course of butene oligomerization over MFI and MTS-3 catalysts was performed by in situ infrared spectroscopy on self-supported wafers, according to the method depicted by Jolly et al. [35]. The catalysts were first saturated with CD_3CN (3 kPa) at room temperature, and then evacuated at 293–403 K in order to regenerate 10 to 30% of the initial acid sites. The sample was cooled at room temperature and the cell equilibrated with 20 kPa of butene. Spectra were recorded (at room temperature) after various thermal treatments performed up to 523 K without intermediate evacuation.

2.4. Catalytic evaluation

The oligomerization of butene was investigated in a down-flow stainless-steel reactor at 423 K with a nitrogen/1–butene flow containing 17% molar butene, a hydrocarbon space velocity (WHSV) varying between 3 and 9 h^{-1} and a total pressure in the range 1.5–2 MPa. The catalyst bed (100–250 mg, powder form) was activated for 4 h at 773 K under nitrogen flow at atmospheric pressure. The reactor temperature was then decreased to 423 K, and the system pressurized with nitrogen. Butene (1-butene, 99.7% purity, 0.2% *cis* + *trans* 2-butene, 0.1% butane) was then fed using a membrane pump. Analysis of the effluent gases was performed by on-line gas chromatography (the first analysis was performed 10 min after the butene stream was stabilized) and recuperation of the condensable products in a cold trap. The latter were analyzed by combined CG/MS. At the end of the runs, the catalysts were flushed with nitrogen at the reaction temperature and then recovered for characterization.

3. Results

3.1. Catalyst characterization

Table 1 gathers the main physico-chemical characteristics of the six catalysts investigated. The XRD patterns of the three MTS-type solids (hereafter MTS-1, MTS-2 and MTS-3) exhibited the intense signal of the (100) diffraction and the less intense (110) and (200) peaks, characteristic of the hexagonal array of MCM-41

Table 1
Main properties of the catalysts used

Catalyst	Si/Al	Pore diameter (nm)	Pore volume (ml/g)	Surface area (m^2/g)	Acidity		% C^c
					meq/g[a]	$\Delta H^b_{kj/mol}$	
MTS-1	30	1.7	0.32	782	0.065	128	18.8
MTS-2	28	3.1	0.55	704	–	120	23
MTS-3	27	3.2	0.70	987	0.075	130	27
ASA	5.9	3–10	0.37	405	0.68	155	8.3
BEA	26	0.76 × 0.64	0.24	623	0.72	160	17.7
MFI	25	0.56 × 0.53	0.17	400	0.74	165	12

[a] Number of acid sites measured by ammonia TPD.
[b] Initial heat of adsorption of ammonia measured by microcalorimetry.
[c] Amount of carbon residue on the spent catalysts.

materials [1,2]. The samples also featured the type IV reversible nitrogen sorption isotherm typical of ordered mesoporous solids. MTS-1, synthesized using OTMA as surfactant, was characterized by a porosity at the border between micro- and mesopores. The difference in pore volume and surface area between samples MTS-2 and MTS-3 is accounted for by the different wall thickness and the resulting different void fraction, as discussed previously [36].

Several methods have been used to investigate the surface acidity of the catalysts. In the last columns of Table 1 are reported the amounts of acid sites as determined by ammonia TPD and the initial heats of adsorption of ammonia, i.e., the heat of adsorption on the strongest sites, measured by microcalorimetry. From these measurements, two facts are apparent. On the one hand, MTS-type materials exhibit a very low population of acid centers that correspond approximately to only 10% of their total aluminium content, whereas this proportion amounts to 70–90% in the case of zeolites with similar overall compositions. Our previous study using carbon monoxide adsorption at 77 K led to a similar conclusion [22]. On the other hand, the strength of the sites is definitely higher for zeolites and ASA than for the mesoporous solid acids. Concerning this last statement, it has to be mentioned that the acid strength of amorphous silica alumina has been reported to be higher [37], lower [38] or identical [39] to that of MCM-41, suggesting that the mode of preparation and of activation of both materials may be critical for the generation of the active sites.

3.2. Nature of acid sites

The nature of the acid sites on the surface of the MFI and MTS-3 samples was investigated by infrared spectroscopy of adsorbed deuterated acetonitrile. This probe is a weak base and the frequency of the stretching vibration mode of the CN bond is highly sensitive to hydrogen bonding, protonation or coordination [35].

Adsorption of CD_3CN on the MFI catalyst at room temperature led to the disappearance of the signal due to bridging hydroxyl groups and to the development of signals at 2114, 2284 and 2323 cm^{-1} (Fig. 1a). The broad band at ca. 2400 cm^{-1} corresponds to one of the components of the shifted ν(OH) band of hydroxyls strongly H-bound to the probe, splitted by the Evan windows. According to literature data [35], the different signals can be assigned to the stretching vibrations of CD_3 groups ($\nu(CD_3)$, signal at 2114 cm^{-1}) and to ν(CN) vibrations of deuterated acetonitrile interacting with Brönsted (signal at 2284 cm^{-1}) and Lewis (signal at 2323 cm^{-1}) sites. After desorption of the sample at 373 K, the intensity of all the signals decreased, but the relative proportion of the peaks characteristic of the adsorbed base remained the same (Fig. 1b). Adsorption of trace amounts of water to the sample led to a decrease of the intensity of the 2323 cm^{-1} signal,

and to an increase of the one at 2284 cm^{-1}, typical of the transformation of Lewis into Brönsted sites, as it is usually observed.

The adsorption of the probe on MTS at room temperature revealed a much weaker interaction of the base with the surface, since the broad band at 2400 cm^{-1} (Fig. 2a) was not observed, and the band characteristic of the interaction with Brönsted sites was shifted to 2276 cm^{-1}. The latter signal was in fact constituted of two components that became visible after desorption at room temperature (Fig. 2b), one at 2288 cm^{-1} due to interaction with Brönsted sites, and the second at 2270 cm^{-1} attributed to acetonitrile interacting with the surface by weak hydrogen bonding, more likely with silanol groups. Rehydration of the sample with 1.3 kPa water vapor at room temperature resulted in an increase of the intensity of the signals at 2270 and 2288 cm^{-1}, indicating that not only Brönsted sites, but also silanol groups had been generated upon hydration. Moreover, the peak characteristic of Lewis acidity (Fig. 2c) was still detected. Such a behaviour is in line with the high propensity of the surface of MTS to undergo hydrolysis of siloxane bridges [33], and shows that water molecules do not disrupt totally the interaction between Lewis sites and acetonitrile.

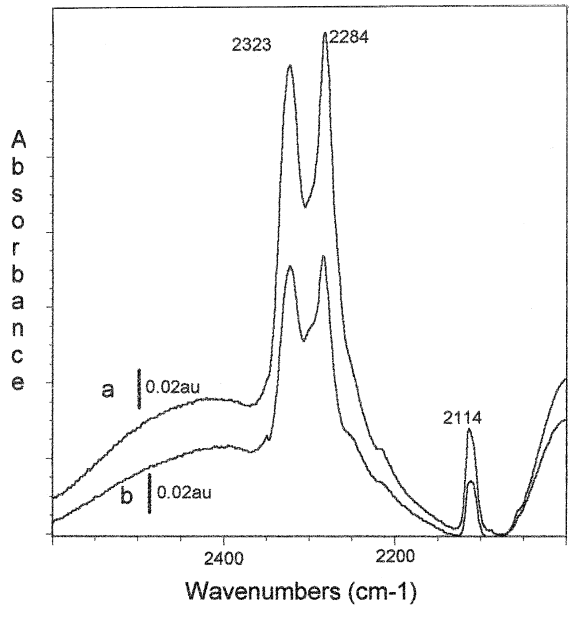

Fig. 1. Infrared spectra of deuterated acetonitrile adsorbed on MFI catalyst. Evacuation temperature: (a) Room temperature, (b) 373 K.

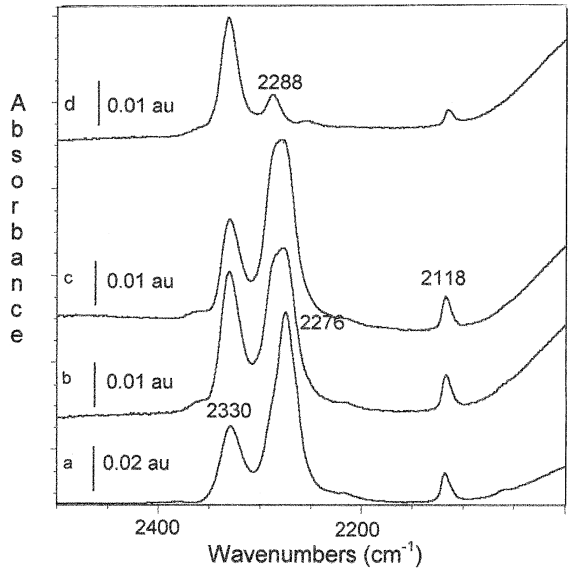

Fig. 2. Infrared spectra of deuterated acetonitrile adsorbed on MTS-3 catalyst. (a) RT adsorption of 3 kPa of base, (b) evacuation at RT, (c) rehydration with 1.3 kPa water vapour, (d) evacuation at 383 K.

After evacuation at 373 K (Fig. 2d), the base interacting with silanol groups was totally removed from the surface, a weak signal characterizing Brönsted sites was still detected, but the main contribution to acidity corresponded to Lewis sites. The latter constitute therefore the strongest sites on the surface of these materials, as previously reported [22].

3.3. Catalytic activity

Fig. 3 compares the catalytic results obtained on the six catalysts at 423 K at a total pressure of 1.9 MPa and with a WHSV of 9 h^{-1}. In these experiments, the conversion corresponds to the amount of butene consumed, and was determined by the difference of its concentration between the inlet and the outlet of the reactor. The results reveal three types of behaviours.

(i) ASA, MFI, and BEA catalysts exhibited a very low initial (after 10 min on stream) activity and became totally inactive after some hours on stream. Only trace amounts of gaseous products other than the butene feed could be detected in these experiments. Additional series of experiments performed at atmospheric pressure on these catalysts allowed to detect reaction products in the effluent stream in the initial stages of the reaction. They consisted of mixtures of linear and branched C_3 to C_{12} paraffins and olefins with odd and even number of carbon atoms, whose formation can be well explained by classical carbenium ion chemistry involving oligomerization, cracking and hydride transfer as elementary steps.

(ii) MTS-2 and MTS-3 showed high initial activity, then deactivated gradually with time on stream and finally led to a nearly constant level of conversion after ca. 10 h reaction. A closer insight into the changes in catalytic behaviour with time on stream is presented by Fig. 4 referring to a run performed using MTS-3 as catalyst, with a WHSV of 4.7 h^{-1} at 1.5 MPa of total pressure. The figure shows that the major process in the initial stages of the reaction was butene oligomerization into residue remaining adsorbed on the catalyst. The products detected at the outlet of the reactor consisted for 85% of branched octenes, including methylheptenes

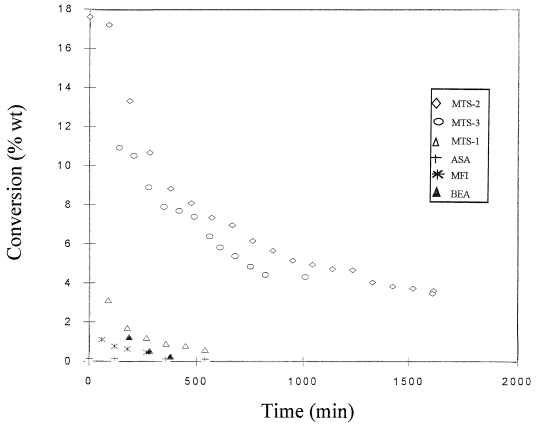

Fig. 3. Conversion of *n*-butene (17% molar in nitrogen) at 523 K, 1.9 MPa and WHSV = 9 h^{-1} on the different catalysts.

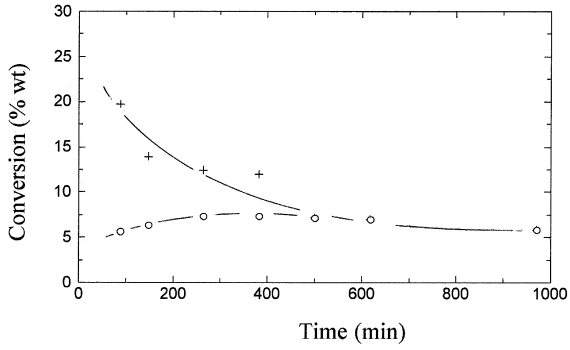

Fig. 4. Conversion of *n*-butene over MTS-3 catalyst. 523 K, 1.5 MPa, WHSV = 4.7 h^{-1}. + Total conversion, 0 Conversion into products.

(10–15%) dimethylhexenes (70–80%) and trimethylpentenes (10–15%) and for 15% of butene trimers. Trace amounts of C_3–C_6 olefinic and paraffinic hydrocarbons (other than the three *n*-butenes that were obtained in amounts approaching thermodynamic equilibrium) were also detected. While increasing time on stream the contribution to residue formation was reduced progressively and, after ca. 8 h on stream, the selectivity into dimers was higher than 98%, the remaining of the products being trimers, and trace amounts of isobutane and isobutene.

(iii) The behaviour of MTS-1 was intermediate between those of the two series of catalysts presented above, in the sense that it exhibited a moderate initial activity and deactivated rapidly (Fig. 3), but the dimerization activity could be still detected after ca. 10 h on stream.

3.4. Nature of the adsorbed oligomers

Dosing the carbon content of the spent catalysts by combined TG/DSC/MS using an oxidizing gas flow (80:20 N_2/O_2 mixture) led to the overall amounts of hydrocarbon residues listed in the last column of Table 1. The mass loss occurred in two steps, in the temperature ranges 473–573 K and 573–823 K, respectively. The first desorption step occurred at a temperature only slightly higher than the reaction temperature, and the products detected in the effluent stream consisted of C_4–C_{12} olefinic

and aliphatic fragments. The weight loss corresponding to this desorption step was the most important in the case of the three MTS-type catalysts, amounting to 60–80% of the total carbon content. In the second desorption step hydrocarbons, including olefinic, aliphatic and aromatic compounds, water and carbon dioxide were formed by a degradation/oxidation process. It has to be noted that most of the hydrocarbon residue of MFI and BEA (80 and 60% of the total carbon, respectively) and the totality of the residue of ASA was degradated during this second step, indicating that the deposits formed in these series of solids were more refractory than those produced on the MTS catalysts.

The difference in the nature of the adsorbed residues on MTS- and zeolite-type catalysts was confirmed by the characterization studies of the spent catalysts MTS-3 and MFI by ^{13}C MAS NMR, infrared and UV–Vis spectroscopies.

The infrared spectra of used MFI and MTS-3 catalysts obtained on self-supporting wafers (outgassed at only 393 K in order to avoid alteration of the residue during sample preparation) are shown in Figs. 5 and 6 for the C–H

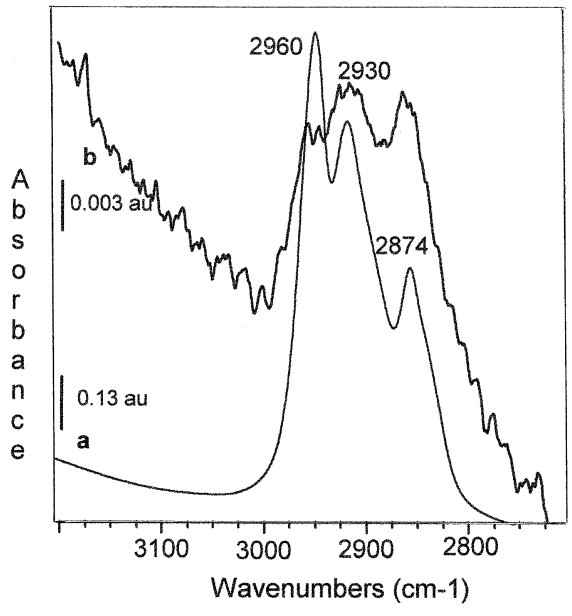

Fig. 5. Infrared spectra in the C–H stretching region of the adsorbed residue on (a) MTS-3 and (b) MFI catalysts.

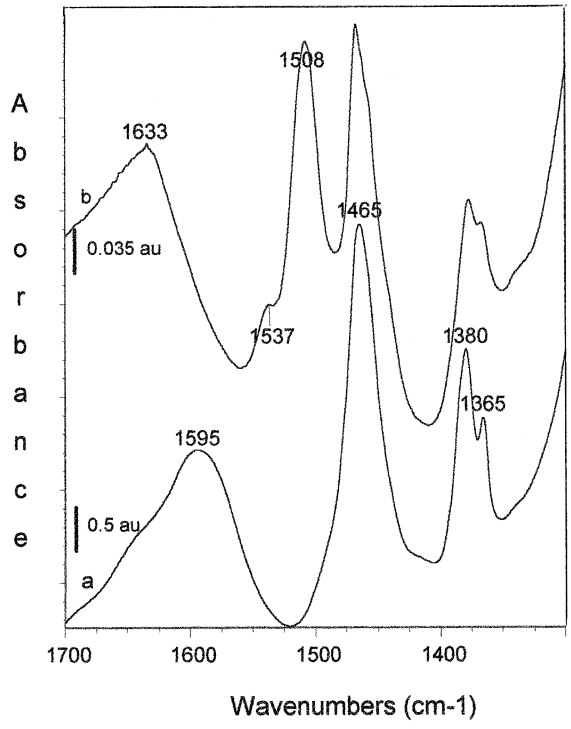

Fig. 6. Infrared spectra of the adsorbed residue on (a) MTS-3 and (b) MFI catalysts.

stretching and deformation regions, respectively. The spectra reveal several features common to both types of catalysts, due to saturated hydrocarbon species, namely CH_3 stretching (2960, 2874 cm^{-1}) and bending modes (1457 cm^{-1}, shoulder), CH_2 stretching (2930 cm^{-1}, 2865 cm^{-1}, shoulder) and bending (1465 cm^{-1}) modes and $C(CH_3)_2$ deformation modes (doublet at 1380 and 1365 cm^{-1}, with the higher frequency band significantly stronger than the lower frequency one). Besides some differences in the relative intensity of the various signals, which suggest a different degree of branching of the hydrocarbon chains (this issue will be discussed later on), signals at 1508 and 1537 cm^{-1} were observed for the MFI sample. The UV–Vis spectrum of the latter exhibited moreover a very intense peak at 298 nm with shoulders at 370 and 450 nm (the three aforementioned UV–Vis signals were also present on the used BEA and ASA catalysts). All these features, which were

absent from the spectra of MTS-3, are characteristic of the presence of conjugated cyclic and/or acyclic allylic carbocations on the used MFI catalyst [40–44]. Finally, on both solids, a broad infrared signal in the region 1600–1650 cm^{-1} due to C=C stretchings was detected. Since no bands attributable to =C–H stretchings (3000–3100 cm^{-1}) were visible, the 1600–1650 cm^{-1} signals can be assigned to substituted olefins or aromatics.

Fig. 7a,b depicts the ^{13}C NMR spectra of used MFI and MTS-3 catalysts recorded using $^{1}H/^{13}C$ cross-polarisation. The spectrum of MTS-3 obtained with $^{13}C/^{1}H$ decoupling is also given in the inset (Fig. 7c). The chemical shifts of the main distinct resonances [45], all corresponding to saturated carbon atoms, are presented in Table 2. As it was already apparent from the previous infrared data, the structure of the strongly adsorbed products formed on the two solids differ significantly, being highly branched for MTS-3 and essentially linear for MFI.

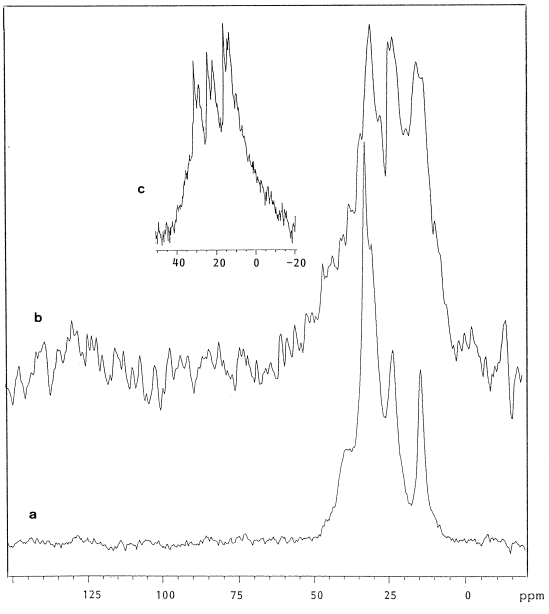

Fig. 7. ^{13}C MAS NMR spectra of the adsorbed residue on MFI (a, CP technique) and MTS-3 (b, CP and c, proton decoupling).

Table 2
Assignment of the main ^{13}C NMR resonances (ppm) of the adsorbed hydrocarbon residue

MTS	MFI
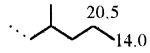	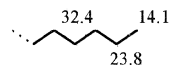
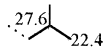	
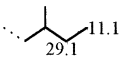	

3.5. In situ characterization of reaction intermediates

Direct observation of aliphatic alkylcarbenium ions inside inorganic matrices such as zeolites has never been reported, probably on account of the insufficient solvating ability of the framework to stabilize these highly reactive species. The recent results by the group of Lavalley in Caen [35] have demonstrated that in the presence of preadsorbed acetonitrile, intermediate carbenium ions could be trapped as stable *N*-alkylnitriliun cations exhibiting infrared ν(CN) vibrations with frequencies specific of the nature, secondary or tertiary, of the carbenium ion involved in the complex. In situ infrared [46,47] and ^{13}C NMR [48] studies demonstrated, moreover, that it was possible to monitor the rearrangements that occur during the reaction of olefins on acidic surfaces. In spite of the difference in the experimental conditions used in the course of in situ studies (static, low partial pressure) and in our catalytic runs (dynamic, high pressure), we used this procedure to further clarify the behaviours of zeolite and MTS-type catalysts during butene oligomerization.

The addition of butene at room temperature to the MTS-3 sample, on which acetonitrile was

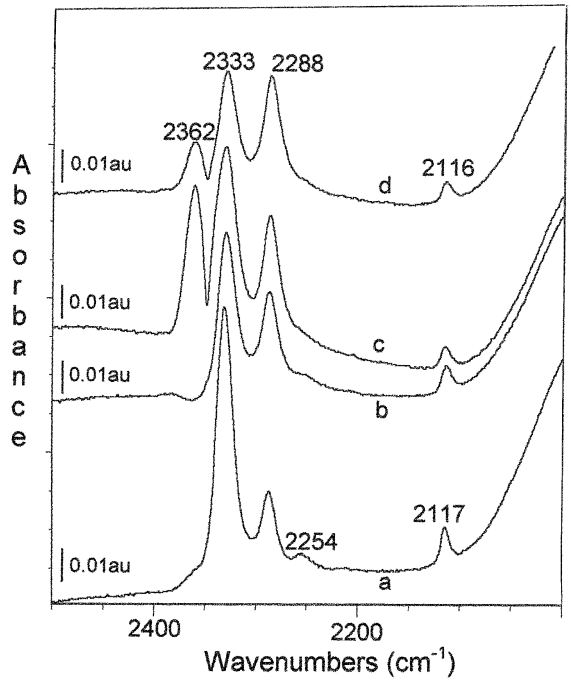

Fig. 8. IR spectra of co-adsorption of CD_3CN and butene over MTS-3. (a) After adsorption and evacuation of CD_3CN, (b) after co-adsorption of butene at RT, (c) heated at 323 K and (d) heated at 423 K.

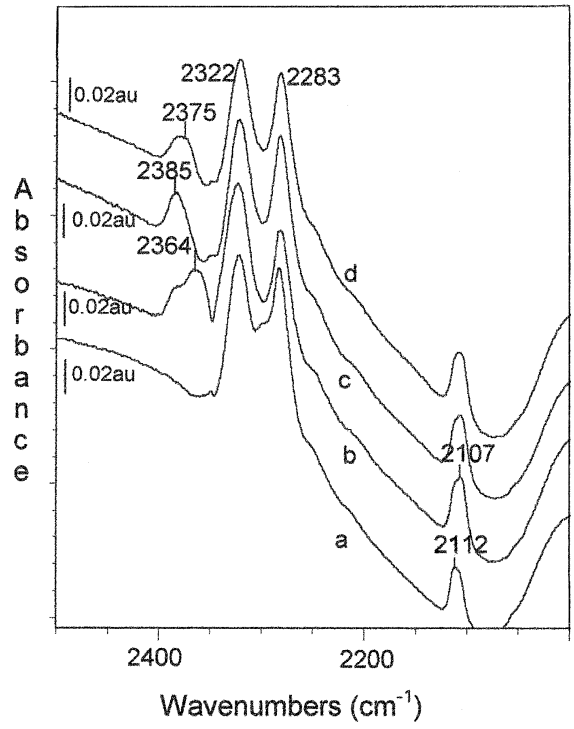

Fig. 9. IR spectra of co-adsorption of CD_3CN and butene over MFI catalyst. (a) After adsorption and evacuation of CD_3CN, (b) after co-adsorption of butene at RT, (c) heated at 323 K and (d) heated at 423 K.

pre-adsorbed, resulted in a slight increase of the proportion of Brönsted sites, which was explained by some hydration of the sample during operation (Fig. 8a,b). No new signal appeared at this temperature. Upon heating to 323 K, a new band at 2362 cm^{-1} developed, assigned to a nitrilium complex involving a tertiary carbenium ion. The formation of tertiary cations is explained by the rapid reaction of the initially formed sec-butyl cations with feed butene molecules to yield branched dimers as shown in Scheme 1.

Further heating of the sample at 373 (not shown) and 423 K (Fig. 8d) affected the relative intensities of the various bands, but did not lead to additional signals in the spectrum, indicating that the growth and rearrangement of the oligomer implied exclusively tertiary carbenium ions as stable intermediates able to react with acetonitrile.

By contrast, the same series of experiments performed on the MFI catalyst revealed a more complex succession of events. Immediately after the addition of the olefin at room temperature, bands at 2364 and 2385 cm^{-1} due to nitrilium complexes involving tertiary and secondary carbenium ions, respectively, became clearly visible (Fig. 9b). Heating for 5 min at 323 K led to an increase of the 2385 cm^{-1} signal and the almost complete disappearance of the one at 2364 cm^{-1} (Fig. 9c). These changes are fully consistent with the rearrangement of a branched dimer or oligomer into a linear one via

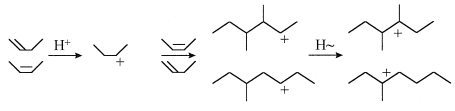

Scheme 1. Formation of tertiary octyl cations.

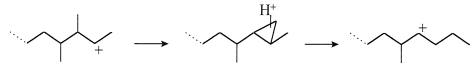

Scheme 2. Change in the degree of branching in carbenium ions.

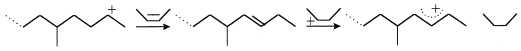

Scheme 3. Formation of allylic cations.

reactions involving protonated cyclopropanes (Scheme 2).

Such a process has been reported previously in the case of infrared [43] and ^{13}C NMR studies of reaction of small olefins or alcohols on acidic MFI-type catalysts, and is believed to be driven by shape-selective effects induced by the narrow pore channels of the zeolite [44–49].

After heating the sample at 373 and 423 K (Fig. 9d), the band initially centered at 2385 cm^{-1} broadened, and its maximum was shifted to lower wave numbers. The position of the maximum fell between those of tertiary and secondary alkylnitrilium cations. A signal in this frequency range has been observed in the case of the adsorption of 1,3-cyclohexadiene on ZSM-5 with pre-adsorbed acetonitrile, while the usual peak at 2385 cm^{-1} was obtained with 1,4-cyclohexadiene (F. Thibault-Starzyk, personal communication, 1997). On the basis of this finding, and owing to the data of Fig. 6b, we can tentatively attribute the spectral changes occurring at high temperature (373–423 K) in our in situ experiments to the formation of allylic cations (Scheme 3).

4. Discussion

The very simple product distributions and the nature of the adsorbed residue observed in the reaction of butene over mesoporous MTS-type materials under experimental conditions where zeolites and classical amorphous silica–alumina do not generate oligomer products in the effluent stream due to fast deactivation must be related to the unique acidic and textural characteristics of this new family of aluminosilicates. Both parameters are believed to exert a positive influence on the activity and stability of the catalysts, and their influences will be discussed below.

4.1. Influence of acidity on catalytic behaviour

The acid-catalyzed transformation of olefins is a classic example of carbenium ion chemistry. Although there may still exist a debate concerning the exact nature of the stable intermediates involved in the reaction process [50,51], the basic steps and sequences of them have been established as early as in the 1930s from studies performed in liquid sulfuric acid. These studies showed that the transformation of light olefins in moderately concentrated acid ($< 75\%$) led exclusively to olefinic dimers and trimers produced via olefin condensation followed by rearrangement of the resulting carbenium ion through hydride and methyl shifts interconverting branched structures and finally deprotonation [52,53]. By contrast, in 96–98% sulfuric acid, the olefins are converted into a complicated mixture of paraffins and cycloolefins by a sequence of oligomerization, rearrangement, cracking, hydrogen transfer and cyclization reactions [54].

From the large amount of knowledge gathered from in situ and ex situ mechanistic and kinetic studies, it is now well established that the very same elementary steps are involved on solid acid catalysts such as crystalline or amorphous aluminosilicates. The extent to which each individual step proceeds depends mainly on acid strength, reaction temperature and catalyst structure in the case of zeolites [44,49,55–57]. Besides gaseous products, the above processes generate bulky, immobile carbonaceous residues, poisoning the active sites and responsible for catalyst deactivation.

The high selectivity into dimers, as well as the aliphatic nature of the adsorbed hydrocarbon residue observed with MTS catalysts, indicate that secondary cracking and bimolecular hydrogen transfer reactions hardly occur on the initially formed carbenium cations. Such a behaviour is typical for a low density of reactive species on the surface, interacting weakly with it. The acidity of the surface of MTS materials is characterized by a moderate strength and a

high dispersion of the sites. Actually, taking into account the surface area developed in the mesopores, and the accessibility of the acidic sites, the density of sites in MTS catalysts is, at least, 10 to 20 times lower than in zeolites and silica–aluminas (Table 1). A low density of weak acid sites well accounts, therefore, for the observed data.

For zeolites and amorphous silica–alumina, the reaction process disclosed in concentrated sulfuric acid has been demonstrated several times and it can be invoked here, albeit no gaseous reaction products were detected. This particular fact can be explained by the experimental conditions we used which favor condensation and hydrogen transfer reactions (the latter leading to refractory compounds) at the expense of cracking, this process being the most activated one in the sequence of events taking place on the surface. This proposal is supported by recent results obtained in the reaction of propene oligomerization showing that MFI-type zeolite catalysts exhibit an activity level comparable to that of mesoporous aluminosilicates (but with a different selectivity, since a broad range of hydrocarbons with only moderate branching was obtained) at significantly higher temperature (by about 100 K), i.e., under conditions where cracking can proceed at a significant rate [29,30].

4.2. Influence of texture

One main peculiarity of the catalytic data reported in this work is the preservation of a stable dimerization activity of mesoporous MTS-type catalysts in spite of the high content of hydrocarbon residue retained on their surface under steady-state conditions. The deactivating effect of the strongly adsorbed hydrocarbon residue can be due to site coverage and pore blockage [58–60]. Assuming that the residue has a density of 0.75 g/ml (a value intermediate between those of octenes and dodecenes), the amounts of carbon dosed on the spent catalysts lead to the conclusion that nearly all the void volume of the microporous catalysts (MTS-1, MFI, BEA) becomes filled with residue in the early stages of the reaction, whereas half of it remains accessible in the case of the mesoporous catalysts MTS-2 and MTS-3. The lack of activity of the former can be therefore readily explained by pore blockage, while the availability of some residual free acid sites could account for the activity of the latter. Such an explanation would mean that the hydrocarbon residue would form as patches on the surface, on account to the large distance between acid centers, rather than lining the mesopore walls. Another alternative which could be invoked is a contribution of the oligomer itself to the process of dimerization. Consecutive alkylation, isomerization, β-scissions reactions, all involving facile type A elementary rearrangements [61,62] between tertiary carbenium ions, occurring on the adsorbed hydrocarbon chain could lead to octene products, as depicted in Scheme 4. Such a mechanism would also explain the formation of trimethylpentenes from *n*-butenes avoiding the intermediate participation of secondary carbenium ions and protonated cyclopropanes.

Whatever the mechanism actually operating, the difference in activity between MTS-1 on the one hand, and MTS-2 and MTS-3 on the other, highlights the positive influence of the open porosity of mesoporous catalysts, since adsorption and desorption of feed molecules and reagents is restricted in the former because of

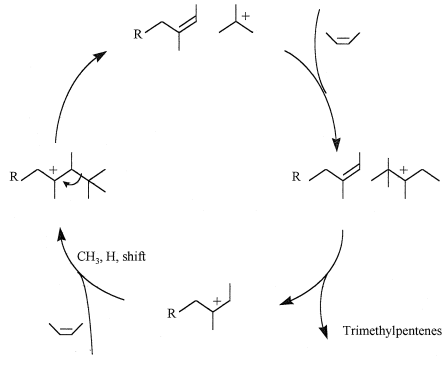

Scheme 4. Formation of trimethylpentenes by oligomer rearrangement and cracking.

pore blockage, whereas no such limitation exist in the latter.

It should be kept on mind, however, that despite textural characteristics close to those of MTS-type materials, the amorphous (classical) silica–alumina catalyst severely deactivated under our experimental conditions. In that case a mechanical effect of the residue cannot be put forward and site coverage by refractory, strongly adsorbed species appears as more likely. As discussed above, the nature of the hydrocarbon residue is determined by the operating conditions, but also by the acid characteristics. A high density of strong sites on the surface of ASA would indeed promote hydrogen transfer reactions, and the formation of a more toxic residue than in the case of MTS-type catalysts.

Without neglecting any positive influence of an ordered mesopore size distribution on the catalytic behaviour of aluminosilicates, our data would emphasize therefore a prominence of the acid properties over the textural ones.

5. Conclusion

Ordered mesoporous aluminosilicates of the MTS-type convert selectively butenes into a mixture of branched dimers at 423 K under a total pressure of 1.5–2 MPa. The catalysts show good stability with time on stream. Under the same experimental conditions, microporous solid acid catalysts are almost totally inactive due to rapid pore blockage by hydrocarbon residue, whereas classical amorphous silica alumina also deactivates by accumulation of immobile hydrogen-poor residue that covers the active sites.

The moderate strength and the low density of sites on the surface of MTS catalysts are probably the main factors responsible for the observed catalytic behaviour. These unique acid characteristics, in the absence of diffusional limitations due to an open porosity, would result in a low concentration of reactive species on the surface with short residence times, and favour deprotonation and desorption of the octyl cations, thus preventing secondary reaction of the olefinic products. The chemical nature of the residue adsorbed on MTS catalysts, which contains highly branched, reactive aliphatic hydrocarbon chains, could also explain the formation of some of the octene dimers.

Acknowledgements

The authors thank Dr. A. Auroux for the microcalorimetry measurements and R. Dutartre and R. Durand for technical assistance and discussions.

References

[1] J.S. Beck, J.C. Vartuli, W.J. Roth, M.E. Leonowicz, C.T. Kresge, K.D. Schmitt, C.T.-W. Chu, D.H. Olson, E.W. Sheppard, S.B. McCullen, J.B. Higgins, J.L. Schlenker, J. Am. Chem. Soc. 114 (1992) 10834.
[2] C.T. Kresge, M.E. Leonowicz, W.J. Roth, J.C. Vartuli, J.S. Beck, Nature 359 (1992) 710.
[3] S. Inagaki, Y. Fukushima, A. Okada, T. Kurauchi, K. Kuroda, C. Kato, Proc. 9th International Zeolite Conference, Montreal, 1992, p. 305.
[4] S. Inagaki, Y. Fukushima, K. Kuroda, J. Chem. Soc., Chem. Commun. (1993) 680.
[5] T. Yanagisawa, T. Shimizu, K. Kuroda, C. Kato, Bull. Chem. Soc. Jpn. 63 (1990) 988.
[6] P.T. Tanev, T.J. Pinnavaia, Science 267 (1995) 865.
[7] D.M. Antonelli, J.Y. Ying, Angew. Chem. Int. Ed. Engl. 35 (1996) 426.
[8] R. Mokaya, W. Jones, J. Chem. Soc., Chem. Commun. (1996) 981.
[9] Q. Huo, R. Leon, P.M. Petroff, G.D. Stucky, Science 268 (1995) 1324.
[10] S.A. Bagshaw, E. Prouzet, T.J. Pinnavaia, Science 269 (1995) 1242.
[11] A. Galarneau, A. Barodawalla, T.J. Pinnavaia, Nature 374 (1995) 529.
[12] A. Sayari, I. Moudrakovski, C. Danumah, C.I. Ratcliffe, J.A. Ripmeester, K.F. Preston, J. Phys. Chem. 99 (1995) 16373.
[13] A. Corma, M.T. Navarro, J. Pérez-Pariente, F. Sánchez, Stud. Surf. Sci. Catal. 84 (1994) 69.
[14] O. Franke, J. Rathousky, G. Schulz-Ekloff, J. Stárek, A. Zukal, Stud. Surf. Sci. Catal. 84 (1994) 77.
[15] P.T. Tanev, M. Chibwe, T.J. Pinnavaia, Nature 368 (1994) 321.
[16] D. Zhao, D. Goldfarb, J. Chem. Soc., Chem. Commun. (1995) 875.
[17] J.-B. Kim, T. Inui, Catal. Lett. 36 (1996) 255.

[18] A. Tuel, S. Gontier, Chem. Mater. 8 (1996) 114.
[19] C.-F. Cheng, H. He, W. Zhou, J. Klinowski, J.A. Sousa Gonçalves, L.F. Gladden, J. Phys. Chem. 100 (1996) 390.
[20] N. Ulagappan, C.N.R. Rao, J. Chem. Soc., Chem. Commun. (1996) 1047.
[21] M. Busio, J. Jänchen, J.H.C. van Hooff, Microporous Mater. 5 (1995) 211.
[22] F. Di Renzo, B. Chiche, F. Fajula, S. Viale, E. Garrone, Stud. Surf. Sci. Catal. 101 (1996) 851.
[23] E. Armengol, M.L. Cano, A. Corma, H. Garcia, M.T. Navarro, J. Chem. Soc., Chem. Commun. (1995) 519.
[24] A. Cauvel, G. Renard, D. Brunel, J. Org. Chem. 62 (1997) 749.
[25] A. Corma, A. Martinez, V. Martinez-Soria, J.B. Monton, J. Catal. 153 (1995) 25.
[26] S.B. Pu, J.B. Kim, M. Seno, T. Inui, Microporous Mater. 10 (1997) 25.
[27] P.B. Venuto, Stud. Surf. Sci. Catal. 105 (1996) 811.
[28] G. Bellussi, M.G. Clerici, V. Arrigoni, R. Ghezzi, Eur. Pat. 463 673 (1992).
[29] G. Bellussi, C. Perego, A. Carati, S. Peratello, E. Previde Massara, G. Perego, Stud. Surf. Sci. Catal. 84 (1994) 85.
[30] Q.N. Le, R.T. Thomson, G.H. Yokomizo, US Pat. 5 134 241 (1992).
[31] F. Di Renzo, N. Coustel, M. Mendiboure, H. Cambon, F. Fajula, Stud. Surf. Sci. Catal. 105 (1997) 69.
[32] F. Vaudry, F. Di Renzo, P. Espiau, F. Fajula, P. Schulz, zeolites, in press.
[33] A. Cauvel, D. Brunel, F. Di Renzo, E. Garrone, B. Fubini, Langmuir 13 (1997) 2773.
[34] D. McQueen, B.H. Chiche, F. Fajula, A. Auroux, C. Guimon, F. Fitoussi, P. Schulz, J. Catal. 161 (1996) 587.
[35] S. Jolly, J. Saussey, J.C. Lavalley, Catal. Lett. 24 (1994) 141.
[36] N. Coustel, F. Di Renzo, F. Fajula, J. Chem. Soc., Chem. Commun. (1994) 967.
[37] A. Corma, V. Fornes, M.T. Navarro, J. Perez-Pariente, J. Catal. 148 (1994) 569.
[38] J.H. Kim, M. Tanabe, M. Niwa, Microporous Mater. 10 (1997) 85.
[39] C.-Y. Chen, H.-X. Li, M.E. Davis, Microporous Mater. 2 (1993) 17.
[40] I. Kiricsi, H. Förster, J. Chem. Soc., Faraday Trans. 1 84 (1988) 491.
[41] E.D. Garbowski, H. Praliaud, J. Chim. Phys. 76 (1979) 687.
[42] S. Bodoardo, R. Chiapetta, F. Fajula, E. Garrone, Microporous Mater. 3 (1995) 613.
[43] A.K. Ghosh, R.A. Kydd, J. Catal. 100 (1986) 185.
[44] A.G. Stepanov, V.N. Sidelnikov, K.I. Zamaraev, Chem. Eur. J. 2 (1996) 157.
[45] E. Breitmaier, W. Voelter, ^{13}C NMR Spectroscopy, Methods and Applications in Organic Chemistry, Verlag Chemie, Weinheim, 1978.
[46] F. Thibault-Starzyk, M.M. Bettahar, J. Saussey, J.C. Lavalley, Stud. Surf. Sci. Catal. 105 (1997) 925.
[47] F. Thibault-Starzyk, R. Payen, J.C. Lavalley, J. Chem. Soc., Chem. Commun. (1996) 2667.
[48] A.G. Stepanov, M.V. Luzgin, Chem. Eur. J. 3 (1997) 47.
[49] J.P. van den Berg, J.P. Wolthuizen, A.D.H. Clague, G.R. Hays, R. Huis, J.H.C. van Hooff, J. Catal. 80 (1983) 130.
[50] V.B. Kazansky, F. Figueras, L.C. De Menorval, Catal. Lett. 29 (1994) 311.
[51] V.B. Kazansky, R.A. van Santen, Catal. Lett. 38 (1996) 115.
[52] F.C. Whitmore, Ind. Eng. Chem. 26 (1934) 94.
[53] F.C. Whitmore, K.C. Laughlin, J.F. Matuzeski, J.D. Surmatis, J. Am. Chem. Soc. 63 (1941) 756.
[54] V.N. Ipatieff, H. Pines, J. Org. Chem. 1 (1936) 464.
[55] E.E. Wolf, F. Alfani, Catal. Rev. -Sci. Eng. 24 (1982) 329.
[56] M.L. Poutsma, in: J.A. Rabo (Ed.), Zeolite Chemistry and Catalysis, Chap. 7, ACS Monograph 171, Am. Chem. Soc., Washington DC, 1976, p. 714.
[57] F. Fajula, F.G. Gault, J. Catal. 68 (1981) 291, 312, 329.
[58] L.D. Rollmann, J. Catal. 47 (1977) 113.
[59] M. Guisnet, P. Magnoux, Appl. Catal. 54 (1989) 1.
[60] G.F. Froment, Stud. Surf. Sci. Catal. 6 (1980) 1.
[61] J. Weitkamp, P.A. Jacobs, J.A. Martens, Appl. Catal. 8 (1983) 123.
[62] D.M. Brouwer, H. Hogeveen, Rec. Trav. Chim. 89 (1970) 211.